

Reactions of Ferrocenium Hexafluorophosphate with P–OR Nucleophiles Give Ring C–H Functionalization or Ring Replacement Products Depending on the Phosphorus Reagent

Aleksandr A. Chamkin,^[a] Vasily V. Krivykh,^[a] Arkady Z. Kreindlin,^[a] Fedor M. Dolgushin,^[a, b, c] and Nikolai A. Ustynuk^{*[a]}

Ferrocenium hexafluorophosphate reacts with different P–OR nucleophiles (PR₃) in CH₂Cl₂ at room temperature to give either half-sandwich complexes [CpFe(PR₃)₃](PF₆) (PR₃=P(OMe)₃, P(OEt)₃, PhP(OMe)₂) or ferrocenylphosphonium salts [CpFe(C₅H₄PR₃)](PF₆) (PR₃=iPr₂P(OMe), iPr₂P(OEt)). Mixtures of both products are formed for some other nucleophiles (PR₃=Ph₂P(OMe), Ph₂P(OEt), PhP(O*i*Pr)₂). The mechanism of the former reaction was established using DFT calculations. This reaction pathway is especially characteristic of π-acceptor nucleophiles,

which is presumably explained by their ability to stabilize the 19e intermediates. The result of the reaction with tertiary phosphines, aminophosphines, and P–OR nucleophiles can be reliably predicted based on the values of the Tolman electronic parameter (below 2070 cm⁻¹ – only ferrocenylphosphonium salt, in between 2073 cm⁻¹ and 2080 cm⁻¹ – only half-sandwich complex, and in the range from 2070 cm⁻¹ to 2073 cm⁻¹ – mixtures of both products).

Introduction

It has been known for almost 70 years that ferrocenium salts can undergo radical substitution reactions. These include alkylation,^[1] cyanalkylation,^[2,3] arylation,^[2,4–7] acylation,^[8] and azolation.^[9] However, the mechanistic details of the C–H bond breaking have never been studied for such processes; therefore, the type of the leaving group (H^{*} or H⁺) remains unclear. The reactions of ferrocenium with neutral and anionic nucleophiles are much less studied. These reactions usually result in complete decomposition of the sandwich ferrocenium structure and formation of [FeX₄]⁻ (X=Cl, Br) or [FeL_n]²⁺ (L=DMF, DMSO, HMPTA, *o*-phen, bipy) complexes.^[10]

Recently we have found two novel reactions of ferrocenium salts with phosphorus nucleophiles. The first one results in the substitution of Cp-ring hydrogen under the action of tertiary phosphines^[11,12] and aminophosphines.^[13] The other reaction is the replacement of the Cp ring itself with secondary phosphines to afford the half-sandwich complexes [CpFe(R₂PH)₃]⁺.^[14] In the course of our study, we have shown that the hydrogen

substitution reactions proceed as an oxidative nucleophilic substitution in ferrocene (Scheme 1), which includes consecutive stages of nucleophilic *exo*-addition of a phosphine (a), redox transformation of IM1 involving the initial ferrocenium salt (b), and the final deprotonation (c).

The direct reaction of ferrocenium with phosphines is the first clear example of an oxidative nucleophilic substitution of hydrogen in a transition metal π-complex. It should be noted that a slight change in the structure of a phosphorus reagent (for instance, replacement of a tertiary phosphine with a secondary one) dramatically alters the reaction outcome: complexes [CpFe(R₂PH)₃]⁺ form instead of the expected ferrocenylphosphonium salts [CpFeC₅H₄PHR₂]⁺.^[14] To the best of our knowledge, the formation of half-sandwich complexes from ferrocenium salts has no precedents.

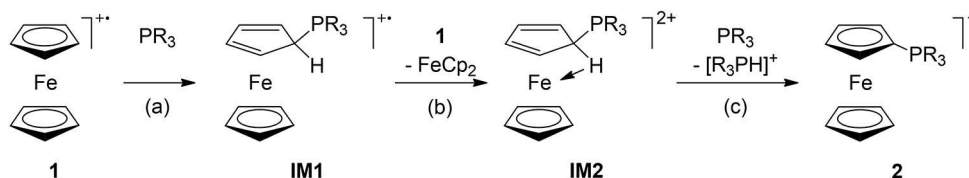
In the present study, we report on a systematic investigation of the reactions of ferrocenium hexafluorophosphate with various P–OR nucleophiles (phosphites, phosphonites, and phosphinites). We showed that these reactions can proceed either as the Cp-ring replacement or C–H functionalization (Scheme 1) depending on the electronic properties of the phosphorus reagent. Finally, we studied the mechanism of the Cp-ring replacement reaction using computational chemistry approaches and showed it to proceed as the initial *exo*-addition of the phosphorus nucleophile to the Cp ring followed by a number of interconversions of 17e and 19e intermediates and a final redox step.

[a] Dr. A. A. Chamkin, Dr. V. V. Krivykh, Dr. A. Z. Kreindlin, Dr. F. M. Dolgushin, Prof. Dr. N. A. Ustynuk
A.N. Nesmeyanov Institute of Organoelement Compounds of Russian Academy of Sciences,
28 Vavilova St., 119991 Moscow, Russian Federation
E-mail: ustynuk@ineos.ac.ru

[b] Dr. F. M. Dolgushin
Kurnakov Institute of General and Inorganic Chemistry of Russian Academy of Sciences,
31 Leninsky prosp., 119991 Moscow, Russian Federation

[c] Dr. F. M. Dolgushin
Plekhanov Russian University of Economics,
36 Stremyanny per., 117997 Moscow, Russian Federation

Supporting information for this article is available on the WWW under <https://doi.org/10.1002/ejic.202100153>



Scheme 1. Substitution of Cp-ring hydrogen under the action of tertiary phosphines and aminophosphines (PR₃).

Results and Discussion

Preparative experiments

Ferrocenium hexafluorophosphate reacts with P–OR nucleophiles of the general formula P(OR)_nR'_{3–n} (n = 1–3) at room temperature (r.t.) in CH₂Cl₂ (Scheme 2, hereinafter counterions are omitted for clarity). The reaction affords different products depending on the nature of the nucleophile (Table 1). The first outcome is the ring C–H functionalization leading to a ferrocenylphosphonium salt (2), the other one involves the replacement of Cp ring to give a half-sandwich complex (3). For some nucleophiles (d–f), the reaction results in both 2 and 3 simultaneously.

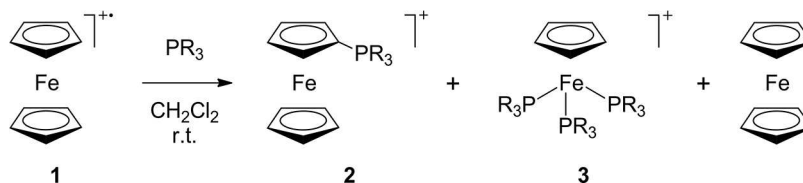
The conversion of ferrocenium is accompanied by a change in the solution color from deep blue to orange, which is useful for determining the reaction completion time when varying the ratio of reagents. For instance, the reactions with phosphinites *i*Pr₂P(OMe) and *i*Pr₂P(OEt) afford only ferrocenylphosphonium salts (2g,h) in high yields and require an equivalent amount of the phosphorus nucleophile in accordance with known stoichiometry (Scheme S1). This is the pathway described by us earlier for tertiary phosphines and aminophosphines (Scheme 1).^[11,13] To be sure of the reaction completion, a small excess of the nucleophile proved to be useful (Table 1).

On the contrary, the reactions with P(OMe)₃, P(OEt)₃, and PhP(OMe)₂ result only in half-sandwich products 3a–c. We assume that the formation of 3 is governed by the stoichiometry

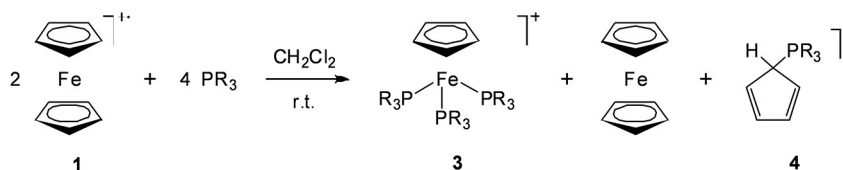
given in Scheme 3, i.e. two equivalents of the phosphorus nucleophile are required to complete the reaction. However, it should be noted that a two-fold excess of the P donor is needed to achieve good yields of 3a and 3b. The reaction with P(OPh)₃ does not proceed at all even with a high excess of the phosphite (Table 1).

Finally, the reactions with Ph₂P(OMe), Ph₂P(OEt), and PhP(O*i*Pr)₂ afford mixtures of 2 and 3, which cannot be readily separated. In accordance with the stoichiometries given in Scheme 3 and Scheme S1, two equivalents of a phosphorus nucleophile are enough for ferrocenium to be fully converted in these cases. The ratio of 2 and 3 changes significantly after the workup: the ferrocenylphosphonium salts 2 are less stable than the half-sandwich complexes 3 and partially degrade during column chromatography. This degradation is complete for 2f. At the same time, the ratio of 2 and 3 does not change when a higher excess of the phosphorus reagent was used. Thus, the reaction with 4.4 or 16 equivalents of Ph₂P(OEt) does give approximately the same yields of 3e. Moreover, the complexes 3 are stable towards substitution of phosphorus ligands. In this way, the treatment of the mixture of 2e and 3e with the excess of P(OEt)₃ does not afford 3b according to ³¹P{¹H} NMR spectroscopy.

As stated above, only half of the initial ferrocenium can be converted into 2 or 3 regardless of the product type (Scheme 3 and Scheme S1). The other half of ferrocenium acts as an oxidizer to result in the formation of ferrocene. Ferrocene was



Scheme 2. General scheme for the reaction of ferrocenium with P–OR nucleophiles with all possible products shown. The transcript of P donors (PR₃) is given in Table 1.



Scheme 3. Stoichiometry of the formation of half-sandwich products 3. The transcript of P donors (PR₃) is given in Table 1.

Table 1. Reagents and yields for the reactions shown in Scheme 2. The yields are given assuming that one mole of the initial ferrocenium salt can produce a maximum of 0.5 moles of either **2** or **3** together with 0.5 moles of ferrocene.

Entry	PR ₃	Yield of 2	Yield of 3	Reaction time	Amount of PR ₃
a	P(OMe) ₃	–	44%	4 h	4.4 eq.
b	P(OEt) ₃	–	28%	4 h	4.4 eq.
c	PhP(OMe) ₂	–	70%	3 h	2.2 eq.
d	Ph ₂ P(OMe)	15% ^[a,b]	12% ^[a,b]	6 h	2.2 eq.
e	Ph ₂ P(OEt)	2.6% ^[b]	2.3% ^[b]	6 h	2.2 eq.
f	PhP(O <i>i</i> Pr) ₂	unstable	traces	1 h	2.2 eq.
g	<i>i</i> Pr ₂ P(OMe)	75%	–	1.5 h	1.1 eq.
h	<i>i</i> Pr ₂ P(OEt)	77%	–	1.5 h	1.1 eq.
i	P(OPh) ₃	–	–	24 h	10 eq.

[a] According to NMR analysis of the reaction mixture. [b] Unseparated.

isolated from the reactions **a**, **c**, and **d** in yields of 64, 70, and 80%, respectively.

Quasi-phosphonium salts **4** (i.e. phosphonium salts, which have at least one phosphorus-heteroatom bond) depicted in Scheme 3 are typically unstable even if they contain only one P–O bond.^[15] Both recorded ³¹P{¹H} NMR spectra of the reaction mixtures in CH₂Cl₂ for P(OMe)₃ and PhP(OMe)₂ display two signals, which can be assigned to known **3a** and **3c** and the corresponding quasi-phosphonium compounds **4a** (δ 52.6) and **4c** (δ 57.7), respectively. Our attempts to isolate **4** failed: the corresponding signal in the spectrum “splits” into many others (e.g. δ 55.3, 57.7, 74.9, 77.6, and 90.5 for **4c**) even after keeping the mixture under argon at r.t. for a day. This comes as no surprise because **4** exists as a mixture of different tautomeric forms, all of which are expected to undergo a fast Diels–Alder reaction. At the same time, the ¹H NMR spectrum in CD₂Cl₂ could not be recorded due to the presence of paramagnetic compounds, which complicated the characterization of **4**.

Despite complexes **2** also being quasi-phosphonium salts, they possess much higher stability than **4**. This is presumably caused by the presence of a ferrocenyl moiety, which partially compensates the positive charge localized on the phosphorus atom. In this way, it acts like aryl groups in the reported stable quasi-phosphonium salts.^[15] The complexes **2g** and **2h** are additionally stabilized by donor isopropyl groups and are

readily isolated in air with the high yields (Table 1), thus showing the greatest stability among the ferrocenylphosphonium salts obtained in the present work. The stability of **2d** and **2e** is lower, so they tend to degrade during the workup. Finally, the complex **2f** is greatly destabilized by the presence of two alkoxy groups and was isolated only in trace yield. Indeed, the presence of weakly nucleophilic counterion (PF₆[−]) is absolutely necessary for the stability of any of these quasi-phosphonium salts. For instance, treatment of **2h** with NaI in (CD₃)₂CO immediately leads to its disappearance (according to ¹H and ³¹P NMR) and the formation of a mixture of unrecognized products.

The structure of cations **2e** and **3e** was determined by X-ray diffraction study of their salts **2e**·PF₆[−] and **3e**·BF₄[−] (Figure 1). The dihedral angle between the two Cp ring planes in cation **2e** is 4.4°. The phosphonium phosphorus displaced by 0.17 Å out of its respective ring plane in a direction away from the Fe atom. Ten Fe–C_{cp} distances show no significant variation with the shortest one of Fe1–C1 2.0246(17), the rest Fe–C distances vary by <0.03 Å. In the P-substituted cyclopentadienyl ring, there is a slight alternation of the C–C bond lengths with slightly elongated C1–C2 and C1–C5 bonds. The P–C_{cp} bond 1.7516(18) Å is visibly shorter than two other P–C_{ph} bonds (1.781(2) Å in average), which is consistent with a partial delocalization of positive charge into the ferrocene fragment. The noted structural features of **2e** coincide with those

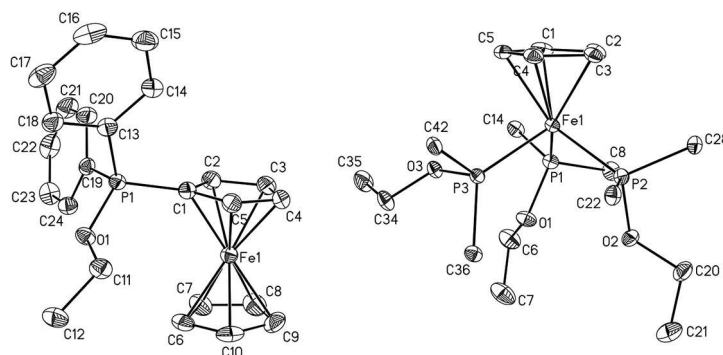


Figure 1. Molecular structures of **2e**PF₆ (left) and **3e**BF₄ (right). Thermal ellipsoids are drawn at the 50% probability level. Hydrogen atoms and counterions are not shown. For **3e**BF₄ two solvation molecules of CH₂Cl₂ are omitted and only C_{ipso} atoms of phenyl groups are shown for clarity. Selected bond lengths (Å) in **2e**: Fe–C_{cp} 2.0246(17)–2.0581(18), P(1)–O(1) 1.5773(12), P(1)–C(1) 1.7516(18), P(1)–C(13) 1.7817(17), P(1)–C(19) 1.7806(18), C(1)–C(2) 1.442(2), C(1)–C(5) 1.444(2), C(2)–C(3) 1.420(3), C(3)–C(4) 1.423(3), C(4)–C(5) 1.412(3). Selected bond lengths (Å) in **3e**: Fe–C_{cp} 2.098(2)–2.125(2), Fe(1)–P(1) 2.2216(7), Fe(1)–P(2) 2.2103(7), Fe(1)–P(3) 2.2361(7), P–O 1.6182(19)–1.6244(18), P–C_{ph} 1.828(3)–1.843(3), C–C_{cp} 1.412(4)–1.429(4).

described earlier for other phosphonium derivatives of ferrocene.^[11,12,16,17]

The half sandwich cation **3e** has a relatively regular three-legged piano stool arrangement (Figure 1) in which the P₃ and C₅ planes are close to parallel with a dihedral angle of 2.9°. Three Fe–P distances are similar to each other and have regular values (ca 2.22 Å). Two OEt (bound to P1 and P2) and one phenyl (bound to P3) substituents are located in an *anti* position relative to Cp ring. The corresponding dihedral angles (X_{Cp}–Fe–P–R, where X_{Cp} stands for the centroid of the Cp ring) are equal to 155.9, 159.9, and 155.7°, respectively. Noteworthy, all the P–O and P–C_{ph} bonds in **3e** are systematically elongated relative to analogous bonds in **2e**. Generally, the structure of **3e** is similar to described structures of other half sandwich cationic complexes of iron with phosphine ligands.^[18–20]

Classification of phosphorus nucleophiles

Inspired by the formation of two totally different products **2** and **3** in the reactions of ferrocenium with different P–OR nucleophiles, we became interested in revealing whether it is possible to reliably predict the outcome of these reactions using some parameter characteristic of the nucleophile. There are two common parameters described for phosphorus (III)

derivatives: the ligand cone angle and the Tolman electronic parameter (TEP).^[21] The ligand cone angle is the measure of the steric bulkiness of a ligand PR₃ in an organometallic complex. This parameter is defined for symmetric ligands as the apex angle of a minimum cylindrical cone, centered 2.28 Å from the phosphorus atom, which just touches the van der Waals radii of the outermost atoms of PR₃. The rigorous definition for asymmetrical ligands can be found elsewhere.^[21] The TEP reflects the electron-donating ability of PR₃. It is defined as the frequency of the A₁ carbonyl mode of (PR₃)Ni(CO)₃ in CH₂Cl₂. The greater is the electron-donating ability of PR₃ the lower is the TEP value. Good additivity of R-group contributions to TEP allows one to estimate its value for ligands for which it has not been measured.^[21]

The values of both Tolman parameters for phosphorus nucleophiles studied earlier^[11,13,14] and in this work are given in Table S1. Figure 2 shows the ligand cone angles plotted against TEPs; the color of points represents the type of the product. This figure gives the impression that the electronic effects are more significant than the steric ones. The TEP scale can be split into three regions: below 2070 cm⁻¹, from 2070 cm⁻¹ to 2073 cm⁻¹, and from 2073 cm⁻¹ to 2080 cm⁻¹, where each region is characterized by the distinct predominance of products of a certain kind. This correlation has no outliers except secondary and primary phosphines (marked with blue

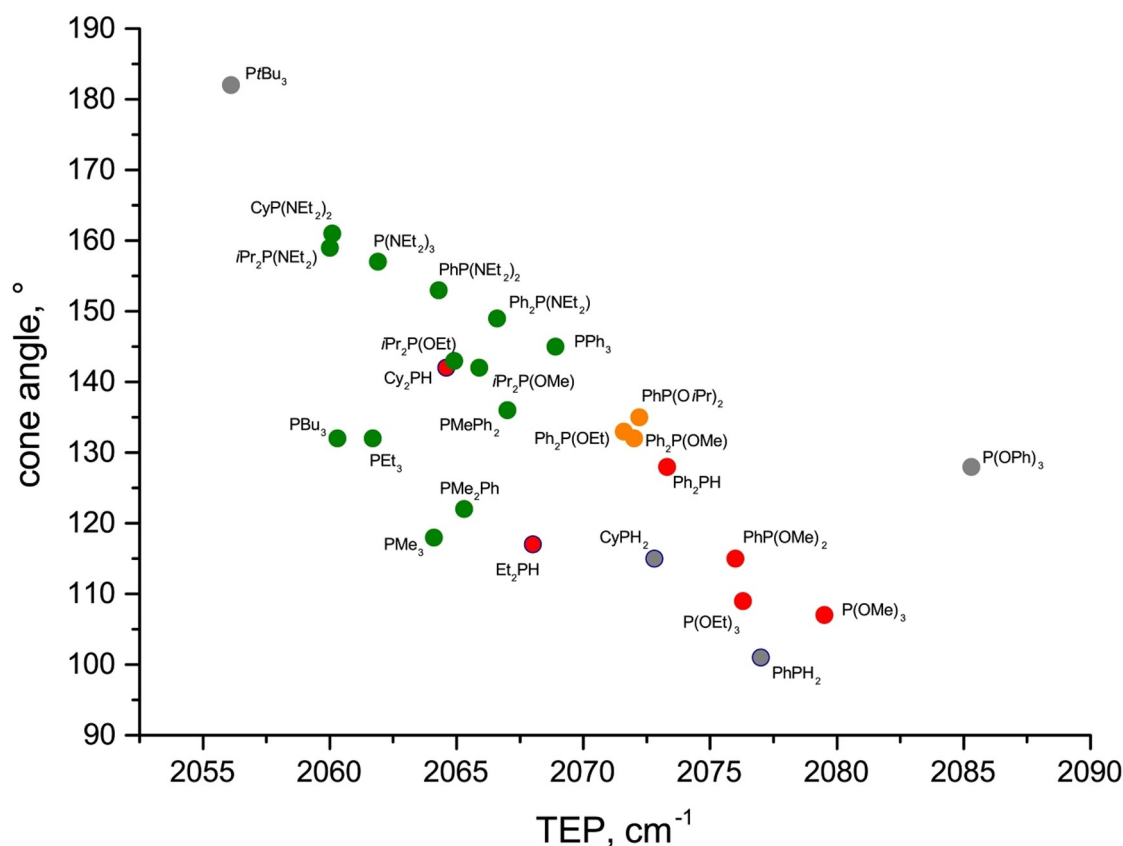


Figure 2. Ligand cone angles plotted against Tolman electronic parameters for different phosphorus compounds. The circle color denotes the type of the product in the reaction with ferrocenium: green circles correspond to **2**, red circles correspond to **3**, orange circles correspond to the mixture of **2** and **3**, and a grey color means no reaction. The blue border denotes an unexpected product. The corresponding data are given in Table S1.

circles in Figure 2). At the same time, there is no correlation with cone angles: for instance, PMe_3 and PhP(OMe)_2 have similar bulkiness but give absolutely different products. The steric bulkiness affects the reaction outcome only in extreme cases. Namely, PtBu_3 is too sterically hindered and, therefore, does not react with ferrocenium. The nonreactivity of other nucleophiles, such as P(OPh)_3 , PhPH_2 , and CyPH_2 , is likely due to their low nucleophilicity.

The Tolman parameters provide the classification of the phosphorus reactants, which is useful for a reliable prediction of the reaction outcome. At the same time, this classification cannot provide an exhaustively accurate prediction, since it does not reveal the mechanistic details of the reactions leading to different products. At this point, more insightful considerations on the reaction mechanisms must be undertaken to reveal why some reaction pathways are unfeasible for certain phosphorus nucleophiles.

Mechanism of the Cp-ring replacement

As was shown above, the reactions of ferrocenium with some P–OR nucleophiles (d,e,g,h) afford ferrocenylphosphonium salts **2**, which suggest these reactions to proceed by the mechanism shown in Scheme 1 similarly to the reactions of ferrocenium

with tertiary phosphines and aminophosphines.^[11,13] This assumption was confirmed by theoretical analysis of the reaction with $i\text{Pr}_2\text{P(OMe)}$ (**g**), in which the thermochemical parameters of the individual steps were found to have very close values to those for PMePh_2 and $\text{PhP(NEt}_2)_2$ as the nucleophiles (Table S3).

On the contrary, the mechanism of the Cp-ring replacement in the reactions with P–OR nucleophiles and secondary phosphines^[14] have never been discussed. Herein, we propose the mechanistic pathway for these reactions shown in Scheme 4. We localized the intermediates and transition states along this pathway for P(OMe)_3 as the nucleophile. The corresponding Gibbs free energy changes and Gibbs free energies of activation are given in Table 2 (hereinafter, the discussion will be related to P(OMe)_3 unless otherwise stated). The energy diagram is shown in Figure 3.

The first reaction step is the *exo*-addition of a P donor to the cyclopentadienyl carbon to form 17-electron (17e) **IM1** (Scheme 4, i). This step can be considered as a redox reaction, in which the formal oxidation state of iron reduces from +3 to +1 and the phosphorus compound oxidizes upon addition. This addition is the most difficult among all other steps in terms of activation energy (Table 2). The corresponding value for P(OPh)_3 is equal to $31.5 \text{ kcal mol}^{-1}$, which explains why this phosphite is not reactive at r.t.

The molecular geometry of **IM1** is shown in Figure S20. The single occupied quasi-restricted orbital^[22] (hereinafter, SOMO) is also depicted for visualization purposes. We assume that the next step of the reaction leading to Cp-ring substitution is the nucleophilic attack of another P–OR molecule on the SOMO, which affords **IM3** (Scheme 4, ii). The formal oxidation state of iron does not change during this process and is equal to +1. However, the resulting **IM3** (Figure S21) is a 19e intermediate and, therefore, a further direct nucleophilic addition to the metal center is impossible.^[23]

The next step is the $\eta^4\text{--}\eta^2$ slippage of the cyclopentadiene ligand in **IM3** (Scheme 4, iii). The resulting 17e **IM4** provides sterically accessible SOMO, which can be attacked by another P donor (Figure S22). The next three reaction steps from this

Step	ΔG°	ΔG_a°
i	19.5	24.2
ii	18.85	18.88
iii	–12.1	5.6
iv	7.0	8.8
v	–15.3	2.5
vi	1.5	~0
vii	–50.0	–
total change	–30.6	–

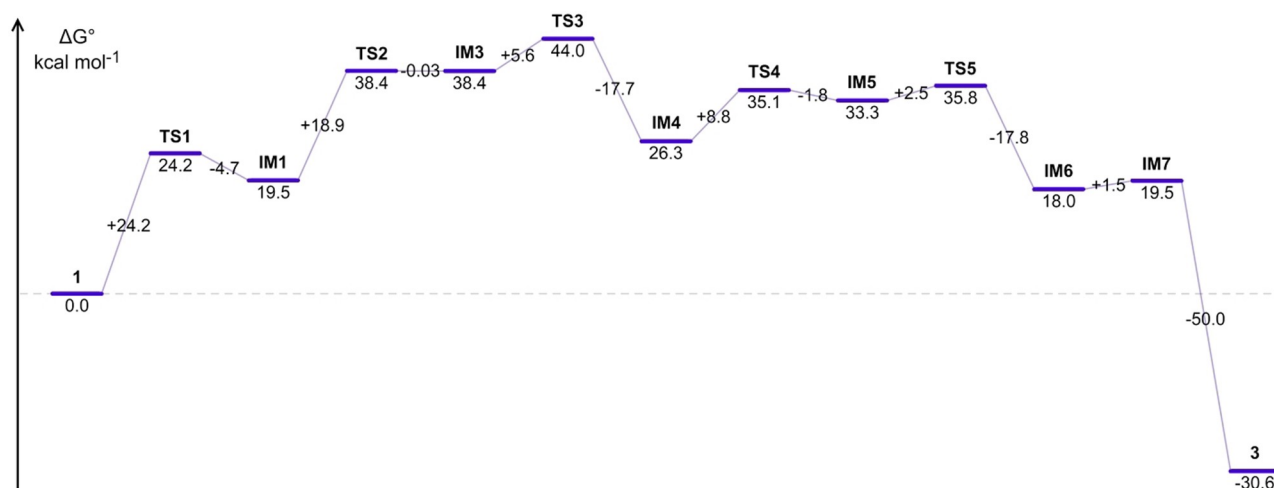


Figure 3. Gibbs free energy change along the reaction coordinate for the Cp-ring replacement reaction with P(OMe)_3 .

point proceed in a similar manner as the addition of a nucleophile molecule to the iron-centered SOMO (Scheme 4, iv), elimination of the cyclopentadiene ligand as **4** (Scheme 4, v), and addition of the third PR₃ to the iron atom (Scheme 4, vi). The latter step (vi) proceeds essentially barrierless and leads to the neutral 19e radical **IM7** (Figure S25).

The final reaction step is the oxidation of **IM7** with the initial ferrocenium (Scheme 4, vii). This step is greatly exothermic ($\Delta G^\circ(\text{vii}) = -50 \text{ kcal mol}^{-1}$), which fully compensates the endothermicity of the preceding steps and makes the whole process feasible. The reaction mechanism described corresponds to the stoichiometry given in Scheme 3, i.e. two molecules of ferrocenium and four molecules of the phosphorus nucleophile act as reagents and afford one molecule of **3**, **4**, and ferrocene.

Discussion of the Cp-ring replacement mechanism

There are three key stages in the mechanism of the Cp-ring substitution reaction. The first one is the *exo*-addition of a P donor (Scheme 4, i). This step is identical for both the C–H functionalization (Scheme 1) and Cp-ring replacement (Scheme 4) reactions. The addition of a phosphorus nucleophile to a coordinated cyclic hydrocarbon ligand is long-known.^[24–26] It is generally accepted that the nature of a P donor (phosphine or phosphite), as well as electrophilicity of the corresponding organometallic complex, are both significant for the feasibility of the addition. In our case, the corresponding activation energies for the *exo*-addition ($\Delta G_a^\circ(\text{i})$) of PMe₃,^[11] P(OMe)₃, and P(OPh)₃ are equal to 16, 24, and 32 kcal mol⁻¹, respectively. So, these values vary greatly from one nucleophile to another, while step i has the highest activation energy among all other steps. Thus, the nature of the P donor determines both the feasibility of its reaction with ferrocenium (regardless of the final product) and the rate of this reaction.

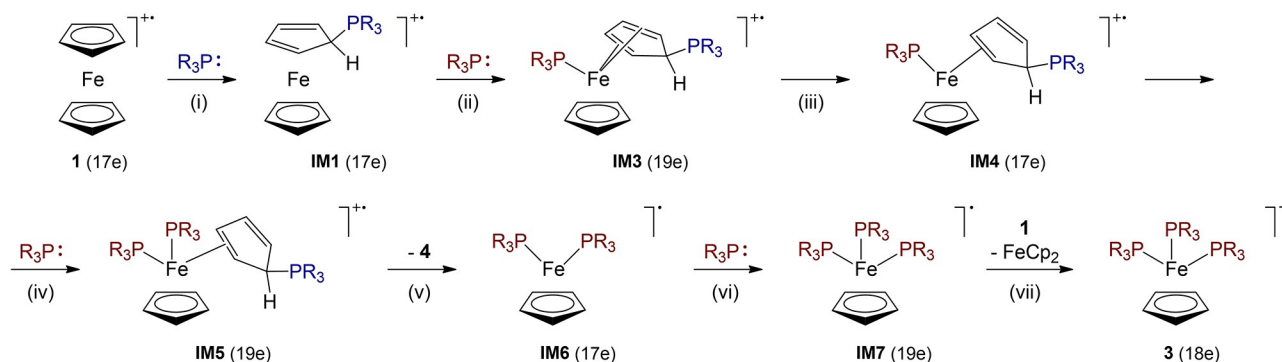
The next part of the Cp-ring substitution reaction is associated with the stepwise addition of the phosphorus nucleophiles to the metal atom and the decooordination of the phosphoniocyclopentadiene ring proceeding as the interconversions of the 17e and 19e intermediates (Scheme 4, ii–vi). The nucleophilic attack occurs at the iron-centered orbital in the 17e intermediates (**IM1**, **IM4**, **IM6**), alternating with slippage of

the cyclopentadiene ring in the 19e intermediates (**IM3**, **IM5**), which reduces the number of valence electrons back to 17.

The consecutive nucleophilic P donor additions have the descending activation energies ($\Delta G_a^\circ = 18.9$, 8.8, and $\sim 0 \text{ kcal mol}^{-1}$ for steps ii, iv, and vi, respectively) and the partial decooordination of the cyclopentadiene ligand follows the same trend ($\Delta G_a^\circ = 5.6$ and $2.5 \text{ kcal mol}^{-1}$ for steps iii and v, respectively). Thus, the addition of the first P donor to the iron atom is more difficult than that for the second and third P donors. It should be emphasized that the elimination of the cyclopentadiene ligand as a spin-paired cation **4** would have been impossible without the initial *exo*-addition to the Cp-ring (Scheme 4, i).

The rapid equilibrium between 17e and 19e “cyclopentadiene-free” complexes **IM6** and **IM7** (Scheme 4, vi) was described for PR₃=PMe₃ and P(OMe)₃ by D. Astruc.^[23] It was shown that in the absence of reducible substrate the 17e form exhibits a radical reactivity (hydrogen abstraction from the medium (THF), the radical Arbusov-Michaelis reaction, or even the radical cleavage of a P–O bond in triphenylphosphite derivatives). On the contrary, an oxidizer can trap the 19e **IM7** via a single-electron redox reaction. This is the case of our reaction: the ferrocenium salt is a perfect oxidizer for **IM7**. So, the final step of the entire process is the redox reaction between **IM7** and the initial ferrocenium to produce both even-electron complex **3** and ferrocene (Scheme 4, vii). This redox process is greatly favored, since the calculated Gibbs free energy change is extremely negative ($-50 \text{ kcal mol}^{-1}$). Additionally, we assume that a two-fold excess of the phosphite is needed to achieve good yields of **3a** and **3b** (Table 1), because it shifts the **IM6**–**IM7** equilibrium to the right thereby hindering the radical side reactions of **IM6**.

The proposed mechanism is based on some established regularities of reactivity of odd-electron organometallic compounds. First of all, the nucleophilic attack on a singly occupied orbital of a 17e complex governs the reactivity of these species. It is accepted that this orbital should be sterically accessible for the interaction to proceed efficiently.^[27] For example, the cyclopentadienyl complex [Cp₂V(CO)]* undergoes CO substitution reactions up to 10⁶ times faster than its pentadienyl analog [(η⁵-C₅H₇)₂V(CO)]*.^[28,29] Both complexes are 17e radicals with similar geometries, molecular orbital levels, electronic effects of



Scheme 4. Mechanism of the formation of the half-sandwich complexes **3**.

ligands, and steric accessibility of the vanadium atom. However, the SOMO of $[(\eta^5\text{-C}_5\text{H}_5)_2\text{V}(\text{CO})]^*$ is oriented mainly towards the $\eta^5\text{-C}_5\text{H}_5$ ligands, whereas the SOMO of $[\text{Cp}_2\text{V}(\text{CO})]^*$ is oriented perpendicular to the plane containing the centroids of Cp and CO ligands.^[30] Our computations give similar shapes for these orbitals (Figure S26 and Figure S27). Thus, the SOMO of the latter complex is sterically accessible for the attack of a nucleophile, which makes the associative substitution mechanism possible. On the contrary, the pentadienyl complex $[(\eta^5\text{-C}_5\text{H}_5)_2\text{V}(\text{CO})]^*$ is far more inert, because the associative mechanism is forbidden in this case.

There are some other reported precedents when the direction of a nucleophilic attack and increased reactivity towards substitution reactions are explained by the shape and orientation of the SOMO (e.g. for $[\text{Mn}(\text{CO})_5]^*$,^[31] $[\text{CpCo}(\text{PETe})_2]^*$,^[32] and $[\text{V}(\text{CO})_6]^*$ ^[33,34]). In our case, the proposed additions of a P donor to the iron atom (Scheme 4, ii, iv, vi) are fully consistent with the above-mentioned trends. In this way, the shapes and orientations of d_{22} -like SOMOs of 17e intermediates (**IM1**, **IM4**, **IM6**) govern the direction of the addition and the geometries of the resulting 19e complexes (Figures S20–S25).

Another concept applicable to the mechanism shown in Scheme 4 is the partial delocalization of the unpaired “19th” electron from the metal center to the phosphorus ligand to

give a *phosphoranyl radical*.^[35] The striking feature of such shifting is the possibility of stabilization of the corresponding 19e intermediate.^[36] The simple interaction of the singly occupied metal orbital with a P donor is shown in Figure 4a. In this case, the unpaired electron occupies the metal-ligand antibonding orbital (σ^*), resulting in a net metal-ligand bond order of $1/2$. However, when a phosphorus nucleophile has a vacant low-energy orbital (A^*), the unpaired electron will be shifted onto it (Figure 4b), which will result in the stabilization of the complex. From this perspective, it becomes clear why the formation of 19e **IM3** (Scheme 4, ii) is possible for $\text{P}(\text{OMe})_3$ but not, for example, for PMe_3 : phosphites possess much higher π -acidity than phosphines because their acceptor orbitals (σ^* orbitals of the P–OR bonds denoted as A^* in Figure 4) lie significantly lower owing to the electron-withdrawing properties of the substituents. Thus, the formation of the corresponding intermediate for PMe_3 is unfavorable (as the result, it cannot be localized computationally). Most likely, this is the main factor that governs the outcome of the reaction for different phosphorus nucleophiles.

Finally, the set of interconversions of 17e and 19e intermediates (Scheme 4, ii–vi), which actually leads to the substitution of one cyclic ligand, is also consistent with the known reactivity pattern for metal radicals. It lies in the fact that such interconversions (“17—19 electron rule”) govern reactions of metal-centered organometallic radicals much in the same way as the 16—18 electron rule governs the reactivity of closed-shell species.^[27,37] The corresponding substitution reactions of 17e complexes usually proceed 10^6 – 10^{10} times faster than for related 18e compounds. For instance, the associative substitution of CO by a phosphorus ligand was described for carbonyl organometallic 17e radicals: $[\text{CpMo}(\text{CO})_3]^*$,^[38–40] $[\text{V}(\text{CO})_6]^*$,^[41,42] $[\text{Re}(\text{CO})_5]^*$,^[43] $[\text{Mn}(\text{CO})_5]^*$,^[44] and $[\text{CpW}(\text{CO})_3]^*$.^[45]

In our case, the proposed mechanism of the substitution of the cyclopentadiene ligand (Scheme 4, ii–vi) is most related to the pentametalation of the arene substitution in 19e $[\text{CpFe}(\text{arene})]^*$ (Scheme 5).^[23,46] This substitution proceeds by a dissociative mechanism, including hapticity lowering of the arene ligand (Scheme 5, a, c, e) and addition of a P donor steps (Scheme 5, b, d). The final 17e intermediate $[\text{CpFe}(\text{PR}_3)_2]^*$ can either undergo

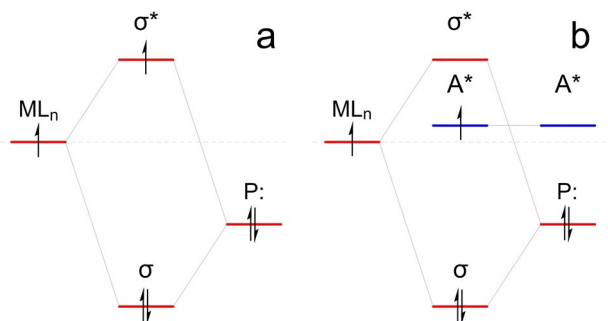
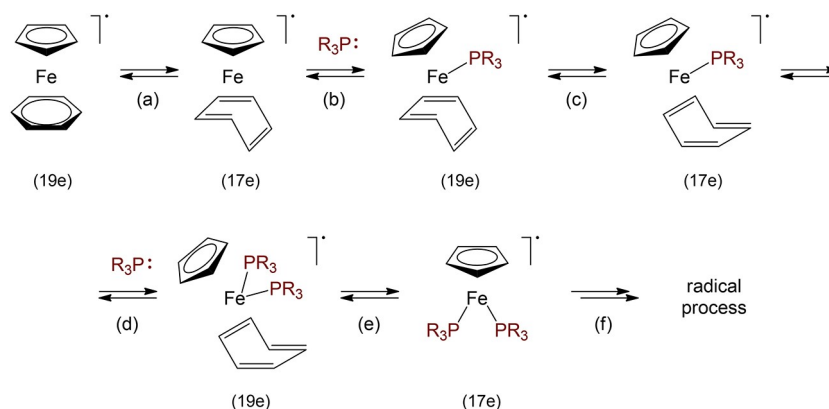


Figure 4. (a) The molecular orbital diagram showing the interaction of the singly occupied metal-centered orbital of a 17e complex (ML_n) with a ligand doubly occupied orbital (P:) to form a pair of bonding (σ) and anti-bonding (σ^*) orbitals of a 19e complex. (b) Same as part a except that the ligand has a low-energy acceptor orbital (A^*).^[36]



Scheme 5. Mechanism of the substitution of the benzene ligand in $[\text{CpFe}(\text{C}_6\text{H}_6)]^*$ in THF ($\text{PR}_3 = \text{PMe}_3, \text{PPh}_3, \text{PPh}_2\text{H}, \text{P}(\text{OMe})_3, \text{P}(\text{OPh})_3$).^[23]

further radical reactions (Scheme 5, f) or another PR_3 addition depending on the reaction conditions (see above). The described substitution process (Scheme 5, a–e) has the first-order kinetics with respect to PR_3 , so the first introduction of a P donor (Scheme 5, either a, b, or c) has the highest activation barrier.^[23] The same trend was observed in our case: the first nucleophilic attack (Scheme 4, ii) has the highest activation energy. Finally, the reactions shown in Scheme 5 proceed smoothly at -20°C , while similar 18e isostructural complexes react only at higher temperatures (e.g. $[\text{CpFe}(\text{C}_6\text{H}_5\text{Cl})]^+$ reacts with $\text{P}(\text{OEt})_3$ at 150°C for 18 h^[47]). Thus, it can be estimated that the corresponding substitution in odd-electron complexes proceeds about 10^9 times faster than in 18e complexes. Following this observation, the reactions of ferrocenium with P–OR nucleophiles studied in the present work proceed in mild conditions too.

As was shown above, the proposed mechanism of the Cp-ring replacement by a P–OR nucleophile is based on some features reported earlier: the substitution itself proceed *via* interconversion of 17e and 19e intermediates, phosphorus reagent attacks the singly occupied metal-centered orbital, and the resulting 19e complexes are stabilized by low-energy acceptor orbitals of a phosphorus ligand. Both ring C–H functionalization and Cp-ring replacement reactions have the common *exo*-addition step (Scheme 1, a and Scheme 4, i, respectively). It can be assumed that **IM1** and **IM2** are always in equilibrium regardless of the nature of a P donor (Scheme 1, b). Therefore, the further reactions are governed by the possibilities of the nucleophilic attack on the SOMO of **IM1** (Scheme 4, ii) to give **IM3** and the deprotonation of **IM2** (Scheme 1, c). For good π -acceptors (phosphites and phosphonites), the former process is feasible due to sufficient stabilization of the corresponding 19e adduct **IM3**. The rate of the 17e–19e substitution is high and, therefore, this process will dominate. On the contrary, for bad π -acceptors (which are usually good bases, e.g. tertiary phosphines and aminophosphines), the intermediate **IM3** is destabilized, so the deprotonation of **IM2** occurs. In some rare cases (d–f), the rates of both processes are similar, so the reaction leads to the formation of both products **2** and **3**. The considerations presented in this Section are in agreement with the classification of the phosphorus reagents by their TEPs presented earlier: thus, the higher value of TEP implies the higher π -acidity of the corresponding PR_3 . However, such a simple classification cannot cover all subtle mechanistic features that govern the outcome in the reactions of ferrocenium with P–OR nucleophiles and cannot provide its absolutely accurate prediction.

Conclusions

Redox activation of organometallic compounds increases their reactivity, which makes possible to carry out those reactions that do not proceed for the initial stable, as a rule, 18e complexes.^[36,37,40,46,48] In the present study, we have found that ferrocenium hexafluorophosphate reacts with P–OR nucleophiles under mild conditions and gives, depending on the P

donor structure, either the ferrocenylphosphonium salts $[\text{CpFeC}_5\text{H}_4\text{PR}_3](\text{PF}_6)$ as the products of ring C–H functionalization or the half-sandwich complexes $[\text{CpFe}(\text{PR}_3)_3](\text{PF}_6)$ as the products of Cp-ring replacement.

Both these reactions are rather complex from the mechanistic point of view; all their key stages are associated with interconversions of odd-electron intermediates. The initial and common for both reactions stage is the nucleophilic addition of the P donor to the cyclopentadienyl ring, which leads to the 17e η^4 -phosphoniocyclopentadiene complex **IM1**. The subsequent addition of the P–OR nucleophile to **IM1** proceeds at the metal atom and leads to the 19e adduct **IM3** stabilized by a partial delocalization of the “19th” electron on the phosphorous ligand. Then, the ring replacement proceeds as alternating processes of the partial decoordination of the η^4 -phosphoniocyclopentadiene ligand and nucleophilic addition of the P donor to the metal; the oxidation of 19e **IM7** by the initial ferrocenium salt completes the formation of half-sandwich product **3**. For bad π -acids, the addition to the metal in **IM1** is energetically unfavorable and the reaction proceeds as its oxidation followed by the deprotonation of the resulting intermediate **IM2**.

Experimental and Computational Section

General Methods: All reactions were performed in an argon atmosphere using Schlenk technique. All workup procedures were performed in air. Organic solvents were dried using standard procedures and distilled prior to use. Commercially available acetylferrocene and phosphites $\text{P}(\text{OMe})_3$, $\text{P}(\text{OEt})_3$, and $\text{P}(\text{OPh})_3$ were used as received. $\text{PhP}(\text{OMe})_2$,^[49] $\text{Ph}_2\text{P}(\text{OMe})$,^[50] $\text{Ph}_2\text{P}(\text{OEt})$,^[51] $i\text{Pr}_2\text{P}(\text{OMe})$, $i\text{Pr}_2\text{P}(\text{OEt})$,^[52] and $\text{PhP}(\text{O}i\text{Pr})_2$,^[53] were prepared according to the published protocols from the corresponding chlorophosphines, dry alcohols, dry triethylamine as a base, and dry petroleum ether as a solvent. Ferrocenium hexafluorophosphate and tetrafluoroborate were prepared as described.^[54] Silica gel (Merck 60, 70–230 mesh) was used for column chromatography. Petroleum ether refers to the 40–70 °C boiling fraction.

NMR spectra were recorded on a Bruker AMX 400 spectrometer in $(\text{CD}_3)_2\text{CO}$ at r.t. using the standard pulse sequences (residual internal $\text{C}_3\text{HD}_5\text{O}$ ($\delta(^1\text{H})$ 2.05), internal $\text{C}_3\text{D}_6\text{O}$ ($\delta(^{13}\text{C})$ 29.84), and external H_3PO_4 85% aq. ($\delta(^{31}\text{P})$ 0). Chemical shifts are given in parts per million (ppm). Elemental analysis was performed on a Carlo Erba 1106 automated CHN analyzer at the Laboratory of Microanalysis of INEOS RAS.

X-ray Diffraction Study: The crystals were grown from dichloromethane/ether by slow diffusion using enriched chromatographic fraction for a given compound. The complex **3e**· $\text{BF}_4 \cdot 2(\text{CH}_2\text{Cl}_2)$ was obtained by the described experimental procedure but using ferrocenium tetrafluoroborate instead of ferrocenium hexafluorophosphate. Single-crystal X-ray diffraction experiments were carried out with a Bruker SMART APEX II diffractometer^[55] (graphite-monochromated Mo K_α radiation, $\lambda = 0.71073 \text{ \AA}$, ω -scan technique). Semiempirical absorption correction based on equivalent reflections was applied using the SADABS program.^[56] The structures were solved by direct methods and refined by the full-matrix least-squares technique against F^2 with anisotropic thermal parameters for non-hydrogen atoms with the SHELXL program.^[57] The hydrogen atoms were placed geometrically and included in the structure factors calculations in the riding motion approximation. Crystallo-

graphic data for complexes **2e**·PF₆ and **3e**·BF₄·2(CH₂Cl₂) are presented in Table S2 in the Supporting Information.

Computational Details: Geometry optimizations were performed without symmetry constraints using the DFT M06-L Minnesota meta-GGA functional,^[58] and tight convergence criteria as implemented in the GAUSSIAN 09 code.^[59] The Pople's split-valence triple-zeta basis set augmented with polarization and diffuse functions 6-311++G(d,p)^[60–66] was used. M06-L functional was chosen because it proved to be accurate for organometallic thermochemistry^[67] and especially for similar molecular systems.^[68] A pruned (99, 590) integration grid (UltraFine) was used. Frequency calculations were performed to confirm the nature of the stationary points to yield one imaginary frequency for the transition states and none for the minima. The reaction path was traced from the transition state to the product and back to the reactant by using the Intrinsic Reaction Coordinate method (IRC).^[69] Thermochemical parameters at 298 K were obtained from frequency calculation by using the same theory level. The solvent corrections for CH₂Cl₂ were applied using the SMD solvation model.^[70] The stability of the DFT wave functions was tested with respect to relaxing^[71] yielding no internal instabilities. Quasi-restricted orbitals were produced in a single-point fashion using the same functional, basis set, and integration grid together with the RI–J approximation with automatically generated auxiliary basis set as implemented in the ORCA 4.0.1 code.^[72] The described effective computational procedures were used to aid the signal assignment in monosubstituted ferrocene derivatives.^[73] The ChemCraft software^[74] was used for molecular visualization.

General Procedure: The corresponding phosphorus compound was added to a solution of ferrocenium hexafluorophosphate in dichloromethane. The reaction mixture was stirred at r.t. until complete disappearance of a deep blue ferrocenium color. The resulting yellow solution was evaporated, the residue was taken up in dichloromethane (1.5 ml) and poured into cold ether (40 ml) with stirring, which resulted in precipitation of products **2** or **3**. The resulting orange solution was decanted off and the residue was washed with cold ether to remove traces of ferrocene. The residue was dried *in vacuo* and purified by column chromatography (1 × 15 cm). The product was eluted with dichloromethane/acetone (5:1), the solution was evaporated, and the residue was reprecipitated from dichloromethane/ether under slow diffusion to yield an analytically pure compound.

Deposition Numbers 2047239 (for **2e**·PF₆), and 2047240 (for **3e**·BF₄·2(CH₂Cl₂)) contain the supplementary crystallographic data for this paper. These data are provided free of charge by the joint Cambridge Crystallographic Data Centre and Fachinformationszentrum Karlsruhe Access Structures service www.ccdc.cam.ac.uk/structures.

Supporting Information

(See footnote on the first page of this article): Full characterization data is given in the Supporting Information.

Acknowledgements

This work was performed with the financial support from Ministry of Science and Higher Education of the Russian Federation using the equipment of Center for molecular composition studies of INEOS RAS.

Conflict of Interest

The authors declare no conflict of interest.

Keywords: Density functional calculations · Ferrocenium cation · Ferrocenylphosphonium salts · Metallocenes · Phosphites

- [1] S. P. Gubin, L. I. Denisovich, N. V. Zakurin, M. G. Peterleitner, *J. Organomet. Chem.* **1978**, *146*, 267–278.
- [2] A. L. J. Beckwith, R. J. Leydon, *Tetrahedron* **1964**, *20*, 791–801.
- [3] V. A. Nefedov, L. K. Tarygina, *Zh. Org. Khim.* **1976**, *12*, 2012–2019.
- [4] G. D. Broadhead, P. L. Pauson, *J. Chem. Soc.* **1955**, 367.
- [5] A. L. J. Beckwith, R. J. Leydon, *J. Am. Chem. Soc.* **1964**, *86*, 952–953.
- [6] V. Weinmayr, *J. Am. Chem. Soc.* **1955**, *77*, 3012–3014.
- [7] M. Rosenblum, W. G. Howells, A. K. Banerjee, C. Bennett, *J. Am. Chem. Soc.* **1962**, *84*, 2726–2732.
- [8] C. Lampard, J. A. Murphy, N. Lewis, *Tetrahedron Lett.* **1991**, *32*, 4993–4994.
- [9] V. N. Babin, Y. A. Belousov, T. A. Belousova, Y. A. Borisov, V. V. Gumenyuk, Y. S. Nekrasov, *Russ. Chem. Bull.* **2012**, *60*, 2081–2087.
- [10] R. Prins, A. R. Korswagen, A. G. T. G. Kortbeek, *J. Organomet. Chem.* **1972**, *39*, 335–344.
- [11] A. A. Chamkin, V. V. Krivykh, O. M. Nikitin, A. Z. Kreindlin, N. A. Shteltser, F. M. Dolgushin, O. I. Artyushin, N. S. Ikonnikov, Y. A. Borisov, Y. A. Belousov, N. A. Ustynyuk, *Eur. J. Inorg. Chem.* **2018**, *2018*, 4494–4504.
- [12] Independently of us, phosphination of a ferrocenium cation with triethylphosphine was described by K. Caulton et al.: B. J. Cook, M. Pink, K. Pal, K. G. Caulton, *Inorg. Chem.* **2018**, *57*, 6176–6185.
- [13] A. A. Chamkin, V. V. Krivykh, N. A. Shteltser, O. V. Semeikin, F. M. Dolgushin, N. A. Ustynyuk, *Russ. Chem. Bull.* **2019**, *68*, 532–539.
- [14] A. A. Chamkin, V. V. Krivykh, N. A. Shteltser, K. I. Utegenov, F. M. Dolgushin, N. A. Ustynyuk, *Russ. Chem. Bull.* **2019**, *68*, 1380–1383.
- [15] H. R. Hudson, *Top. Phosphorus Chem.* **1983**, *11*, 339.
- [16] W. E. McEwen, C. E. Sullivan, R. O. Day, *Organometallics* **1983**, *2*, 420–425.
- [17] P. Kubler, J. Sundermeyer, *Dalton Trans.* **2014**, *43*, 3750–3766.
- [18] D. C. R. Hockless, Y. B. Kang, M. A. McDonald, M. Pabel, A. C. Willis, S. B. Wild, *Organometallics* **1996**, *15*, 1301–1306.
- [19] D. E. Herbert, M. Tanabe, S. C. Bourke, A. J. Lough, I. Manners, *J. Am. Chem. Soc.* **2008**, *130*, 4166–4176.
- [20] H. Brunner, H. Kitamura, T. Tsuno, *Organometallics* **2017**, *36*, 2424–2436.
- [21] C. A. Tolman, *Chem. Rev.* **1977**, *77*, 313–348.
- [22] F. Neese, *J. Am. Chem. Soc.* **2006**, *128*, 10213–10222.
- [23] J. Ruiz, M. Lacoste, D. Astruc, *J. Am. Chem. Soc.* **1990**, *112*, 5471–5483.
- [24] P. J. Domaille, S. D. Ittel, J. P. Jesson, D. A. Sweigart, *J. Organomet. Chem.* **1980**, *202*, 191–199.
- [25] D. A. Sweigart, *J. Chem. Soc. Chem. Commun.* **1980**, *23*, 1159.
- [26] Y. Keun Chung, E. D. Honig, D. A. Sweigart, *J. Organomet. Chem.* **1983**, *256*, 277–283.
- [27] *Organometallic Radical Processes* (Ed.: W. C. Troglér), Elsevier Science Publishers, Amsterdam and New York **1990**.
- [28] R. M. Kowaleski, F. Basolo, W. C. Troglér, R. D. Ernst, *J. Am. Chem. Soc.* **1986**, *108*, 6046–6048.
- [29] R. M. Kowaleski, F. Basolo, W. C. Troglér, R. W. Gedridge, T. D. Newbound, R. D. Ernst, *J. Am. Chem. Soc.* **1987**, *109*, 4860–4869.
- [30] R. M. Kowaleski, F. Basolo, J. H. Osborne, W. C. Troglér, *Organometallics* **1988**, *7*, 1425–1434.
- [31] R. L. Harlow, P. J. Krusic, R. J. McKinney, S. S. Wreford, *Organometallics* **1982**, *1*, 1506–1513.
- [32] R. L. Harlow, R. J. McKinney, J. F. Whitney, *Organometallics* **1983**, *2*, 1839–1842.
- [33] M. J. Therien, W. C. Troglér, *J. Am. Chem. Soc.* **1988**, *110*, 4942–4953.
- [34] G. F. Holland, M. C. Manning, D. E. Ellis, W. C. Troglér, *J. Am. Chem. Soc.* **1983**, *105*, 2308–2314.
- [35] W. G. Bentrude, *Phosphorus Sulfur Silicon Relat. Elem.* **1977**, *3*, 109–130.
- [36] D. R. Tyler, *Acc. Chem. Res.* **1991**, *24*, 325–331.
- [37] W. C. Troglér, *Int. J. Chem. Kinet.* **1987**, *19*, 1025–1047.
- [38] R. J. Haines, C. R. Nolte, *J. Organomet. Chem.* **1970**, *24*, 725–736.
- [39] R. J. Haines, A. L. Du Preez, I. L. Marais, *J. Organomet. Chem.* **1971**, *28*, 97–104.

- [40] A. E. Stiegman, D. R. Tyler, *Comments Inorg. Chem.* **1986**, *5*, 215–245.
- [41] Q. Shi, T. G. Richmond, W. C. Trogler, F. Basolo, *J. Am. Chem. Soc.* **1982**, *104*, 4032–4034.
- [42] Q. Z. Shi, T. G. Richmond, W. C. Trogler, F. Basolo, *J. Am. Chem. Soc.* **1984**, *106*, 71–76.
- [43] A. Fox, J. Malito, A. Poë, *J. Chem. Soc. Chem. Commun.* **1981**, *20*, 1052–1053.
- [44] T. R. Herrinton, T. L. Brown, *J. Am. Chem. Soc.* **1985**, *107*, 5700–5703.
- [45] N. N. Turaki, J. M. Huggins, *Organometallics* **1986**, *5*, 1703–1706.
- [46] D. Astruc, *Acc. Chem. Res.* **1991**, *24*, 36–42.
- [47] C. C. Lee, U. S. Gill, M. Iqbal, C. I. Azogu, R. G. Sutherland, *J. Organomet. Chem.* **1982**, *231*, 151–159.
- [48] D. Astruc, *Chem. Rev.* **1988**, *88*, 1189–1216.
- [49] E. Bergin, C. T. O'Connor, S. B. Robinson, E. M. McGarrigle, C. P. O'Mahony, D. G. Gilheany, *J. Am. Chem. Soc.* **2007**, *129*, 9566–9567.
- [50] C. U. Grunanger, B. Breit, *Angew. Chem. Int. Ed.* **2008**, *47*, 7346–7349; *Angew. Chem.* **2008**, *120*, 7456–7459.
- [51] P. A. Spreider, B. Breit, *Org. Lett.* **2018**, *20*, 3286–3290.
- [52] N. I. Rinehart, A. J. Kendall, D. R. Tyler, *Organometallics* **2018**, *37*, 182–190.
- [53] D. J. Collins, P. F. Drygala, J. M. Swan, *Aust. J. Chem.* **1983**, *36*, 2095.
- [54] N. G. Connelly, W. E. Geiger, *Chem. Rev.* **1996**, *96*, 877–910.
- [55] *APEX II software package*, Bruker AXS Inc., 5465, East Cheryl Parkway, Madison, WI 5317 **2005**.
- [56] G. M. Sheldrick, *SADABS, Program for Empirical Absorption Correction of Area Detector Data*, Göttingen University, Göttingen, Germany **2004**.
- [57] G. M. Sheldrick, *Acta Crystallogr. Sect. C* **2015**, *71*, 3–8.
- [58] Y. Zhao, D. G. Truhlar, *J. Chem. Phys.* **2006**, *125*, 194101.
- [59] *Gaussian 09*, Revision E.01, M. J. Frisch, G. W. Trucks, H. B. Schlegel, G. E. Scuseria, M. A. Robb, J. R. Cheeseman, G. Scalmani, V. Barone, B. Mennucci, G. A. Petersson, H. Nakatsuji, M. Caricato, X. Li, H. P. Hratchian, A. F. Izmaylov, J. Bloino, G. Zheng, J. L. Sonnenberg, M. Hada, M. Ehara, K. Toyota, R. Fukuda, J. Hasegawa, M. Ishida, T. Nakajima, Y. Honda, O. Kitao, H. Nakai, T. Vreven, J. A. Montgomery, Jr., J. E. Peralta, F. Ogliaro, M. Bearpark, J. J. Heyd, E. Brothers, K. N. Kudin, V. N. Staroverov, T. Keith, R. Kobayashi, J. Normand, K. Raghavachari, A. Rendell, J. C. Burant, S. S. Iyengar, J. Tomasi, M. Cossi, N. Rega, J. M. Millam, M. Klene, J. E. Knox, J. B. Cross, V. Bakken, C. Adamo, J. Jaramillo, R. Gomperts, R. E. Stratmann, O. Yazyev, A. J. Austin, R. Cammi, C. Pomelli, J. W. Ochterski, R. L. Martin, K. Morokuma, V. G. Zakrzewski, G. A. Voth, P. Salvador, J. J. Dannenberg, S. Dapprich, A. D. Daniels, O. Farkas, J. B. Foresman, J. V. Ortiz, J. Cioslowski, D. J. Fox, Gaussian, Inc., Wallingford CT **2013**.
- [60] A. D. McLean, G. S. Chandler, *J. Chem. Phys.* **1980**, *72*, 5639–5648.
- [61] R. Krishnan, J. S. Binkley, R. Seeger, J. A. Pople, *J. Chem. Phys.* **1980**, *72*, 650–654.
- [62] A. J. H. Wachters, *J. Chem. Phys.* **1970**, *52*, 1033–1036.
- [63] P. J. Hay, *J. Chem. Phys.* **1977**, *66*, 4377–4384.
- [64] K. Raghavachari, G. W. Trucks, *J. Chem. Phys.* **1989**, *91*, 1062–1065.
- [65] T. Clark, J. Chandrasekhar, G. W. Spitznagel, P. V. R. Schleyer, *J. Comput. Chem.* **1983**, *4*, 294–301.
- [66] M. J. Frisch, J. A. Pople, J. S. Binkley, *J. Chem. Phys.* **1984**, *80*, 3265–3269.
- [67] D. G. Gusev, *Organometallics* **2013**, *32*, 4239–4243.
- [68] A. A. Chamkin, E. S. Serkova, *J. Comput. Chem.* **2020**, *41*, 2388–2397.
- [69] K. Fukui, *Acc. Chem. Res.* **2002**, *14*, 363–368.
- [70] A. V. Marenich, C. J. Cramer, D. G. Truhlar, *J. Phys. Chem. B* **2009**, *113*, 6378–6396.
- [71] R. Seeger, J. A. Pople, *J. Chem. Phys.* **1977**, *66*, 3045–3050.
- [72] F. Neese, *WIREs Comput. Mol. Sci.* **2017**, *8*.
- [73] A. A. Chamkin, *Int. J. Quantum Chem.* **2021**, *121*, e26456.
- [74] Chemcraft - graphical software for visualization of quantum chemistry computations. <https://www.chemcraftprog.com>.

Manuscript received: February 22, 2021
 Revised manuscript received: March 23, 2021
 Accepted manuscript online: March 23, 2021